https://doi.org/10.3311/PPci.44806 | 1
Creative Commons Attribution

Periodica Polytechnica Civil Engineering

Effect of Phenocrystic Orthoclase Content on Leeb Hardness Values of Granitic Rocks

Emre Karakaya[1], Mehmet Can Balcı[2*], İsmail İnce[3]

[1] Department of Mining Engineering, Faculty of Engineering and Natural Sciences, Konya Technical University, 42250, Konya, Türkiye
[2] Department of Civil Engineering, Faculty of Engineering and Architecture, Batman University, 72100, Batman, Türkiye
[3] Department of Geological Engineering, Faculty of Engineering and Natural Sciences, Konya Technical University, 42250, Konya, Türkiye
[*] Corresponding author, e-mail: mehmetcan.balci@batman.edu.tr

Received: 19 May 2026, Accepted: 22 June 2026, Published online: 18 July 2026

Abstract
The Leeb hardness (HL) method, which is one of the surface hardness measurement techniques used for materials, has recently gained widespread application in rock mechanics and engineering geology studies. However, limited research has been conducted on the factors influencing HL values. This study aims to investigate the effect of phenocryst-sized minerals on HL values in granitic rocks originating from Türkiye. Within this scope, HL values were determined on 72 surfaces belonging to two different rock types (Kaman Rose and Dusty Rose). Subsequently, high-resolution images obtained from each sample surface were evaluated using image analysis techniques, and the orthoclase mineral percentage (OMP) on the surfaces was quantitatively determined. The relationships between HL and OMP values obtained from the cube sample surfaces of both rock groups were investigated through simple regression analysis, and strong positive linear correlations were identified. The OMP value on the sample surface was determined to be a decisive parameter directly influencing the HL values of the rocks. Textural heterogeneities caused by phenocrysts influenced the HL test results, thereby limiting the applicability of the method to such rock types.

Keywords
Leeb hardness (HL), image processing, phenocrysts, orthoclase mineral percentage (OMP), granite, simple regression

1 Introduction

The Leeb hardness (HL) test was first developed by Dietmar Leeb in 1975 for the practical and non-destructive determination of the hardness of metals and polymers. Over time, owing to its applicability to different material types such as wood, concrete, and rocks, this method has found extensive use in numerous disciplines including geomorphology, civil engineering, restoration studies, materials engineering, engineering geology, and rock mechanics [1–11]. In addition to being a non-destructive technique, the ability to select the impact direction and its broad measurement scale (0-1000) have led to its increasing utilization in rock mechanics and engineering geology studies in recent years [7, 12, 13]. Initial studies in this field mainly focused on identifying relationships between HL values and the strength and physical properties of rocks, such as porosity, dry density, and *P*-wave velocity, as well as strength parameters including uniaxial compressive strength, point load strength index, and Brazilian tensile strength [7, 10–27].

Among the physical properties investigated, the strongest relationship was consistently reported as the negative correlation between porosity and HL values [7, 28–30]. The most intensively studied strength parameter has been the prediction of uniaxial compressive strength. In this context, researchers achieved high correlation coefficients using various approaches including simple regression [7, 14, 17–20, 22–24], multiple regression [16, 21], artificial neural networks [15], and fuzzy logic methods [16].

Recent studies have indicated that HL values are affected by factors such as porosity, rock texture, and mineralogical composition [7, 10, 11, 27–29, 31, 32]. Ghorbani et al. [28, 31] emphasized that increasing pore and crack density in rocks

Cite this article as: Karakaya, E., Balcı, M. C., İnce, İ. "Effect of Phenocrystic Orthoclase Content on Leeb Hardness Values of Granitic Rocks", Periodica Polytechnica Civil Engineering, 2026. https://doi.org/10.3311/PPci.44806

leads to decreasing HL values and broader standard deviation ranges in the measurements. Several researchers reported that increasing porosity adversely affects the performance of the HL device [29, 30]. Furthermore, some researchers highlighted that significant deviations in HL test results occur when the hardness values of the constituent rock components are distributed over a wide range [7, 27, 29, 31]. İnce and Bozdağ [7] also reported that coarse grains or large crystals within rocks may cause substantial deviations in HL measurements. Balcı and İnce [32] identified a strong positive correlation (R^2 = 0.90) between the percentage of volcanic rock fragments in pyroclastic rocks and HL values. Similarly, İnce et al. [10] reported a strong negative correlation (R^2 = 0.92) between pumice content and HL values, whereas a strong positive correlation (R^2 = 0.95) was observed between volcanic lithic fragments and HL values.

Determining the effect of phenocrysts on the HL values of rocks is important for evaluating the applicability and reliability of HL standards developed for rock materials. Although several studies have investigated the influence of lithic fragments and pumice content on HL measurements, no study has directly examined the relationship between phenocryst percentage on sample surfaces and HL values. Therefore, in the first stage of this study, the phenocryst percentages on cube sample surfaces obtained from two different granites exhibiting wide variations in phenocryst content were determined using image processing software (Image Pro Plus 6.0), and their correlation with HL values was investigated.

2 Material and method

2.1 Material

In this study, commercially exploited granitic rocks containing coarse orthoclase crystals obtained from two different regions of Anatolia were used. Macro- and micro-scale images of the rocks are presented in Fig. 1, while their macro- and microscopic descriptions are summarized in Table 1 [33].

Sample No. 1 was obtained from the Kaman district of Kırşehir Province and is commercially known as "Kaman Rose." The rock is light grey in color and composed of medium to coarse grained crystals. Quartz, plagioclase, and hornblende phenocrysts constitute the principal mineral phases. In addition, large pink-colored orthoclase crystals with long axes reaching approximately 3–4 cm are distinctly observed. Macroscopic investigations

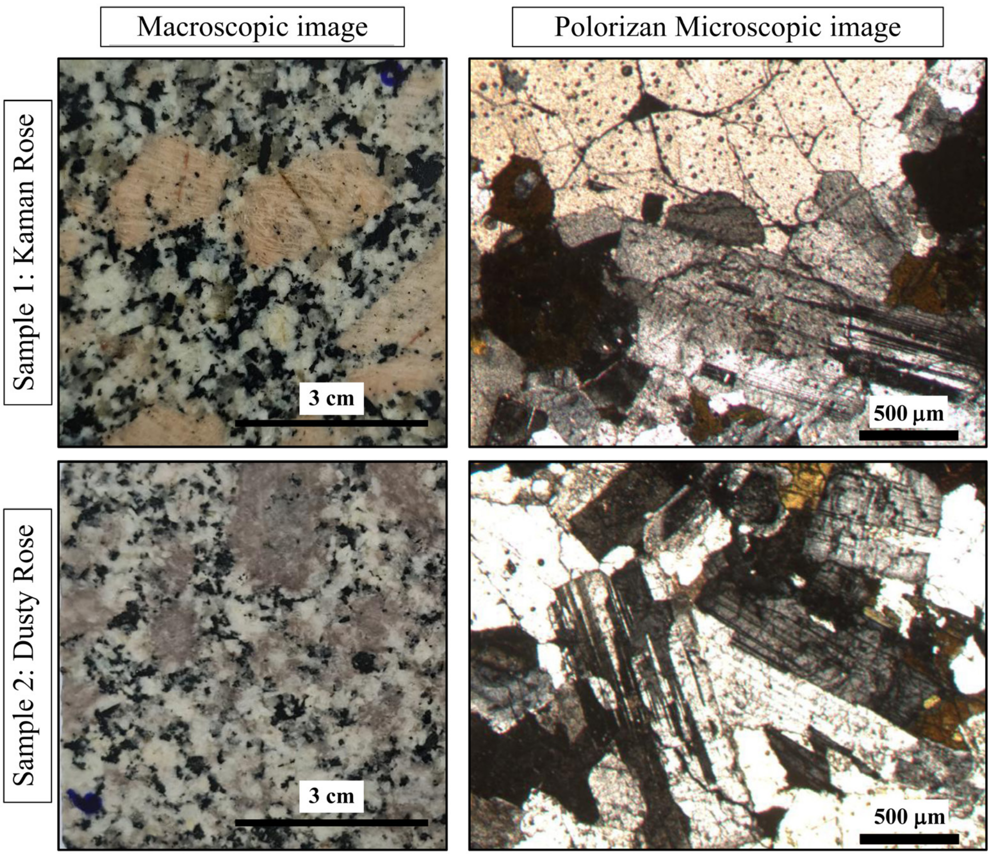

Fig. 1 Macro and micro views of the granitic rock samples

Table 1 The textural characteristics and mineralogical compositions of the plutonic rocks used in the study

Sample No	Macro properties		
	Rock components	Colour	Texture
1 (Kaman Rose)	Q, P, O, H	Light grey	Medium-grained, coarse-grained, phono-crystalline, porphyritic texture
2 (Dusty Rose)	Q, P, O, H	Light grey	Medium-grained, coarse-grained, phono-crystalline, porphyritic texture
Sample No	**Micro properties**		
	Mineralogical composition	Texture	Rock name*
1 (Kaman Rose)	O: 33, P: 26, Q:20, H:14, B:5, Om:2	Porphyritic	Granit
2 (Dusty Rose)	O: 35, P: 28, Q:17, H:13, B:6, Om:1	Porphyritic	Granit

B: biotite, H: hornblende, O: orthoclase, Om: opaque mineral, P: plagioclase, Q: quartz, *Rock names given according to Streckeisen [33]

revealed the development of a phaneritic-porphyritic texture. Petrographic thin-section analyses indicated that the rock consists of orthoclase (33%), plagioclase (26%), quartz (20%), hornblende (14%), biotite (5%), and opaque minerals (2%). Sample No. 2 was obtained from Ulaş district of Kırıkkale Province and is commercially referred to as "Dusty Rose." This rock is also light grey and composed of medium- to coarse-grained crystals. Medium-grained quartz, plagioclase, and hornblende phenocrysts are present together with rose-colored coarse orthoclase crystals whose long axes reach approximately 2 cm. Macroscopic investigations revealed a phaneritic-porphyritic texture. Polarized microscope analyses showed that the rock consists of orthoclase (35%), plagioclase (28%), quartz (17%), hornblende (13%), biotite (6%), and opaque minerals (1%). According to the mineralogical composition, both rocks were classified as "granite" based on the classification of Streckeisen [33]. However, considering their pronounced porphyritic textures, the rocks were more specifically defined as "granite porphyry".

2.2 Method

Block samples were collected to determine the mineralogical and petrographic characteristics, physical properties, and HL values of the granitic rocks. Subsequently, six cubic samples with edge lengths of 7 cm were prepared for each rock group in accordance with the procedures recommended by TS EN-1936 [34] (Fig. 2(a)). Using these cube samples, the physical properties of the rocks, including porosity and dry density, were determined following the methodology proposed in TS EN-1936 [34]. During these measurements, sample volumes were determined using a caliper, while dry and saturated masses were measured using a precision balance (Figs. 2(b) and 2(c)). *P*-wave velocity (V_p) values were determined according to the procedures recommended in ASTM E494-10 [35].

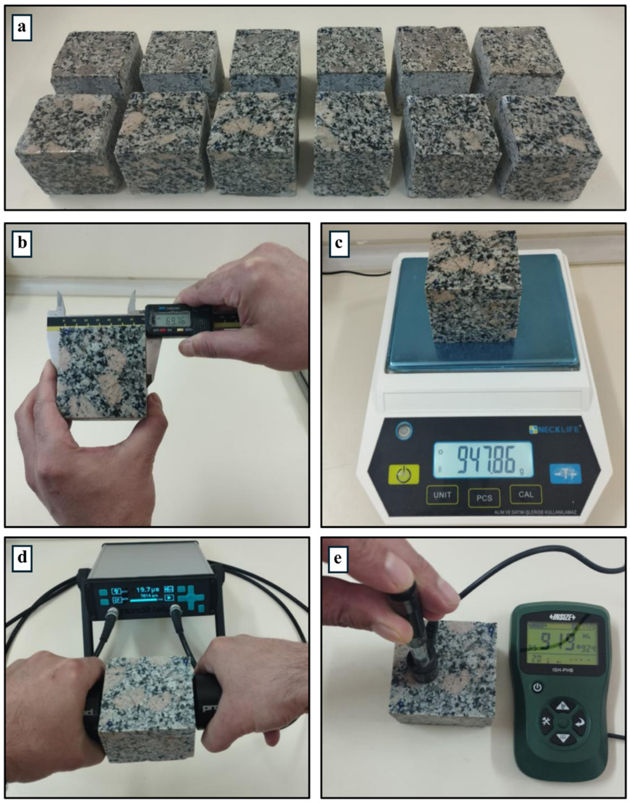

Fig. 2 (a) Cubic samples prepared from rocks; measurement of certain physical properties of the rocks, (b) dimension measurement, (c) dry weight measurement, (d) P-wave velocity, (e) HL

A Proceq Pundit PL-200 device was used for the measurements (Fig. 2(d)). The device consists of two transducers (transmitter and receiver) and a measurement unit. Prior to testing, the instrument was calibrated, and ultrasonic gel was applied between the sample and the transducers to improve contact quality. The direct transmission method was employed for *P*-wave velocity measurements, and measurements were repeated six times for each rock group. The average of these measurements was considered as the representative *P*-wave velocity of the samples.

HL is defined as a dynamic or rebound-type surface hardness parameter associated with both the plastic and elastic characteristics of the tested material [36]. The HL value is obtained by transferring the energy generated by a spring force to a spherical tungsten impact body, allowing the impact body to strike the sample surface at a constant velocity, and calculating the ratio between impact and rebound energies multiplied by 1000 [36]. Although the HL test was originally developed for steel products and standardized under ASTM A956 [36], no standardized procedure has yet been established for rock materials. Therefore, in this study, the approach proposed by İnce and Bozdağ [7] and Balcı and İnce [32] was adopted. Accordingly, HL values were determined as the arithmetic mean of measurements obtained from 20 different points on each sample surface. HL measurements were performed using an Insize-brand HL tester equipped with a *D*-type probe having an impact energy of 11 Nmm (Fig. 2(c)). The *D*-type probe has a diameter of 3 mm and provides measurements within a range of 0-999 HL with an accuracy of ±6 HL. The measurement accuracy of the device, specified as ±6 HL, constitutes a source of uncertainty that should be taken into account when interpreting the results. Nevertheless, it should be recognized that the variability observed in HL values may not solely be attributed to the measurement system, but may also be influenced by the mineralogical composition, textural characteristics, and the associated heterogeneous nature of the rocks. Prior to testing, the device was calibrated using a standard calibration block. To investigate the influence of orthoclase mineral content on HL values, HL measurements were separately determined for each surface of the prepared cube samples. For each surface, HL was measured at 20 randomly selected points, and the average value was accepted as the representative HL value of that surface. In total, measurements were conducted on 36 surfaces (6 cube samples × 6 surfaces) for each granite type.

High-resolution photographs of each granite sample surface were captured using a 45-megapixel Canon EOS R5 camera in order to quantify the orthoclase mineral content. Following image acquisition, the areal percentage of orthoclase crystals larger than 7 mm^2 was determined for each cube surface. This threshold value was selected to represent the effective contact area of the *D*-type impact probe. The quantitative distribution of orthoclase minerals was analysed using Image Pro Plus 6.0 image-processing software. The boundaries of orthoclase phenocrysts were manually identified and delineated based on the mineralogical and textural characteristics observed in the images. The "range" and "smooth" parameters used during the analysis were determined by considering the values at which the boundaries between the phenocrysts and the matrix could be most clearly distinguished in the images. While the "range" parameter contributed to enhancing contrast differences, the "smooth" parameter was used to reduce irregularities along the boundary lines. All images were evaluated following the same processing steps, and particular attention was paid to maintaining consistency in the measurements. However, since the identification of phenocryst boundaries depends on the petrographic assessment of the researcher, it should be acknowledged that the method may involve a certain degree of user induced variability. All images were evaluated following identical processing procedures to ensure consistency in the measurements. In the subsequent stage, image masking procedures were applied to improve the visualization of the spatial distribution of orthoclase mineral boundaries. Finally, the proportion of the total sample surface occupied by orthoclase minerals was calculated for each surface. Orthoclase phenocrysts smaller than 7 mm^2 were excluded from the evaluation. Orthoclase phenocrysts exhibiting this size were excluded from the evaluation because the impact area was susceptible to matrix effects. Accordingly, the obtained HL values were intended to more accurately represent the mechanical behaviour of the phenocrysts. In addition, petrographic investigations of the igneous rock samples were carried out using thin sections prepared in accordance with the procedures recommended by TS EN-12407 [37]. The prepared thin sections were examined under a Leica DM 2700 P polarized microscope.

3 Results and discussion

The statistical parameters (minimum, maximum, mean, and standard deviation) of the physical properties, including porosity, dry density, and *P*-wave velocity, of the granitic rocks used in this study are presented in Table 2. The average dry density, porosity, and *P*-wave velocity values of the Kaman Rose samples were determined as 2.66 g/cm^3, 0.93%, and 4.63 km/s, respectively. For the Dusty Rose samples, the average dry density, porosity, and *P*-wave velocity values were found to be 2.63 g/cm^3, 1.02%, and 4.73 km/s, respectively. The relatively high standard deviation values observed in the *P*-wave velocity measurements of both granite types are considered to result from variations in the distribution of orthoclase minerals within the samples.

Table 2 Physical properties of rocks and HL values

Rock name	Number of samples	Statistical definition	ρ_d (g/cm^3)	n (%)	V_p (km/s)
Kaman Rose	6	Mean	2.66	0.93	4.63
		Minimum	2.65	0.90	4.42
		Maximum	2.66	0.96	5.12
		Standard deviation	0.01	0.03	0.31
Dusty Rose	6	Mean	2.63	1.02	4.73
		Minimum	2.60	0.96	4.17
		Maximum	2.65	1.06	5.25
		Standard deviation	0.02	0.05	0.39

ρ_d: dry density, n: porosity, V_p: P-wave velocity

During the determination of HL values for the Kaman Rose and Dusty Rose samples, the HL values of orthoclase and the other constituent minerals (plagioclase, quartz, hornblende, etc.) were first measured separately (Table 3). Examination of Table 3 indicates that the minimum HL values of orthoclase and other minerals ranged between 831.50-825.17 and 696.50-719.50, respectively, while the maximum values ranged between 902.25-899.63 and 801.33-821.20, respectively. These findings demonstrate that the primary factor controlling HL variations in random measurements is associated with the size and distribution of orthoclase minerals at the contact point of the impact probe.

To better understand this phenomenon, the distributions of orthoclase mineral percentages determined on different surfaces of the cube samples were analyzed using image processing techniques and evaluated through descriptive statistical methods (Fig. 3, Table 4). Within this framework, the general characteristics of the dataset

Table 3 Statistical characteristics of HL values for minerals in rocks

Rock name	Number of samples	Measurement surface	Number of HL measurements	orthoclase			other minerals		
				Min	Max	SD	Min	Max	SD
Kaman Rose	6	36	720	831.50	902.25	16.07	696.50	801.33	23.44
Dusty Rose	6	36	720	825.17	899.63	15.74	719.50	821.20	19.59

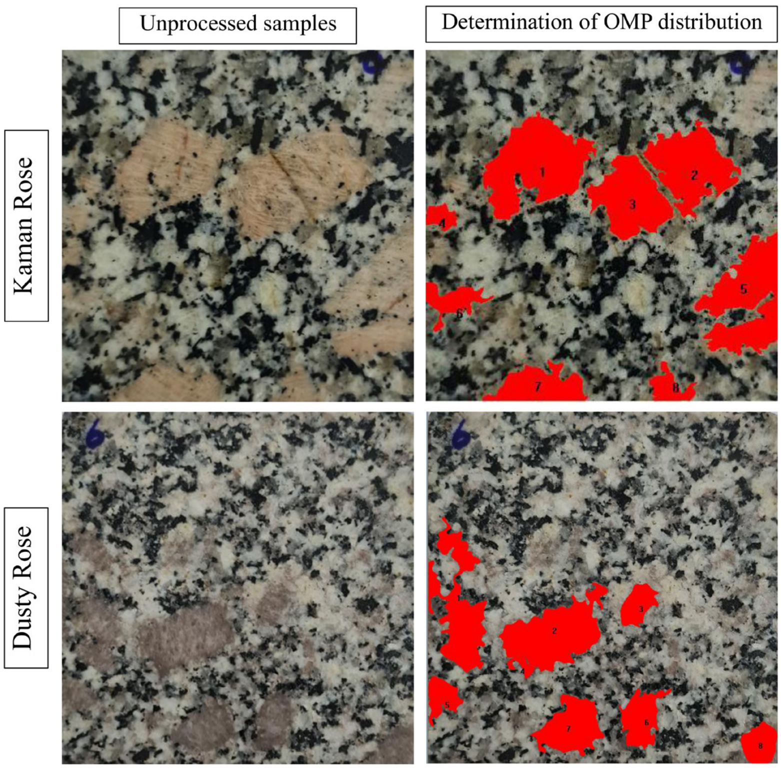

Fig. 3 Determination of OMP on sample surfaces using image processing software

Table 4 Statistical data on the distribution of the percentage values of orthoclase minerals on the surfaces of cube samples

Rock name	Statistical definition			
	Mean	Minimum	Maximum	Standard deviation
Kaman Rose	12.37	2.71	26.00	5.78
Dusty Rose	17.74	5.11	41.04	8.61

were evaluated using mean values together with dispersion parameters such as minimum and maximum values and standard deviations. This statistical assessment enabled quantitative interpretation of the variability in orthoclase content observed between different sample surfaces and provided insight into the homogeneity of the dataset.

As presented in Table 4, the orthoclase mineral percentages (OMP) determined from 72 sample surfaces belonging to 12 cube samples of the two granite groups varied between 2.71% and 41.04%. To evaluate the influence of orthoclase content on HL behaviour, the relationship between the OMP values and the average HL values obtained from 20 randomly selected measurement points on each corresponding surface was analysed using simple regression (SR) analysis. For this purpose, linear, power, exponential, and logarithmic regression models were employed to characterize the nature of the HL-OMP relationship. The statistical reliability of the developed relationships was evaluated using *T*-tests, *F*-tests, coefficient of determination (R^2), adjusted coefficient of determination (Adj. R^2), error metrics (RMSE, MAE, and MAPE), and information criteria (AIC and BIC). The significance of the regression models was assessed at a significance level of $\alpha = 0.05$, and all models with *p*-values lower than 0.05 were considered statistically significant. The validation metrics of the four regression models representing the relationships between HL and OMP for each rock type and for the combined dataset are presented in Table 5, while the corresponding regression plots are shown in Fig. 4.

The regression models developed for the HL-OMP relationships of the Kaman Rose and Dusty Rose samples generally exhibited high predictive performance. The R^2 values ranging between 0.81 and 0.95 demonstrate that OMP is a highly explanatory parameter for HL values. For Kaman Rose and Dusty Rose, the highest correlation coefficients were obtained using linear models, with R^2 values of 0.935 and 0.947, respectively. The exponential models also demonstrated similar performance (R^2 = 0.935 for Kaman Rose and R^2 = 0.945 for Dusty Rose); however, the linear models yielded lower MAE and RMSE values, indicating superior predictive capability. In contrast, the power and logarithmic models showed relatively lower performance and were less successful in explaining HL variations. The *p*-values of all models were lower than 0.001, confirming the statistical significance of the developed relationships.

The results obtained from the combined dataset indicate that the relationship between HL and OMP exhibits a generally strong explanatory capability. The R^2 values ranged approximately between 0.83 and 0.94, with the best performance obtained from the linear model ($R^2 = 0.944$). The exponential model followed closely with an R^2 value of 0.943 and also demonstrated good predictive performance in terms of error metrics. However, the power and logarithmic models again exhibited relatively poor performance and failed to adequately represent the complexity of the relationship. Overall, the findings indicate that the linear structure of the HL-OMP relationship provides a more practical and consistent representation for engineering applications.

Table 5 Performance comparison of regression models for predicting HL from OMP values

Rock Name	Model	R^2	Adj R^2	MAE	RMSE	MAPE (%)	*F*	*p*-value	AIC	BIC
Kaman Rose	Linear	0.935	0.933	2.818	3.348	0.334	490.52	<0.001	193.18	196.35
	Exponential	0.935	0.933	2.801	3.329	0.331	496.19	<0.001	−292.56	−289.40
	Power	0.819	0.813	4.597	5.603	0.545	151.67	<0.001	−254.79	−251.62
	Logarithmic	0.813	0.807	4.648	5.690	0.551	147.66	<0.001	231.35	234.52
Dusty Rose	Linear	0.947	0.946	3.345	4.311	0.393	611.93	<0.001	211.38	214.55
	Exponential	0.945	0.944	3.427	4.381	0.402	577.41	<0.001	−272.97	−269.80
	Power	0.899	0.896	3.989	5.977	0.469	291.33	<0.001	−250.26	−247.09
	Logarithmic	0.892	0.889	4.112	6.160	0.484	282.37	<0.001	237.08	240.24
All Sample	Linear	0.944	0.943	3.062	3.995	0.361	1184.49	<0.001	407.78	412.33
	Exponential	0.943	0.942	3.101	4.035	0.365	1141.19	<0.001	−561.73	−557.18
	Power	0.837	0.835	4.888	6.821	0.577	351.56	<0.001	−485.75	−481.19
	Logarithmic	0.829	0.827	4.995	6.989	0.590	339.92	<0.001	488.32	492.87

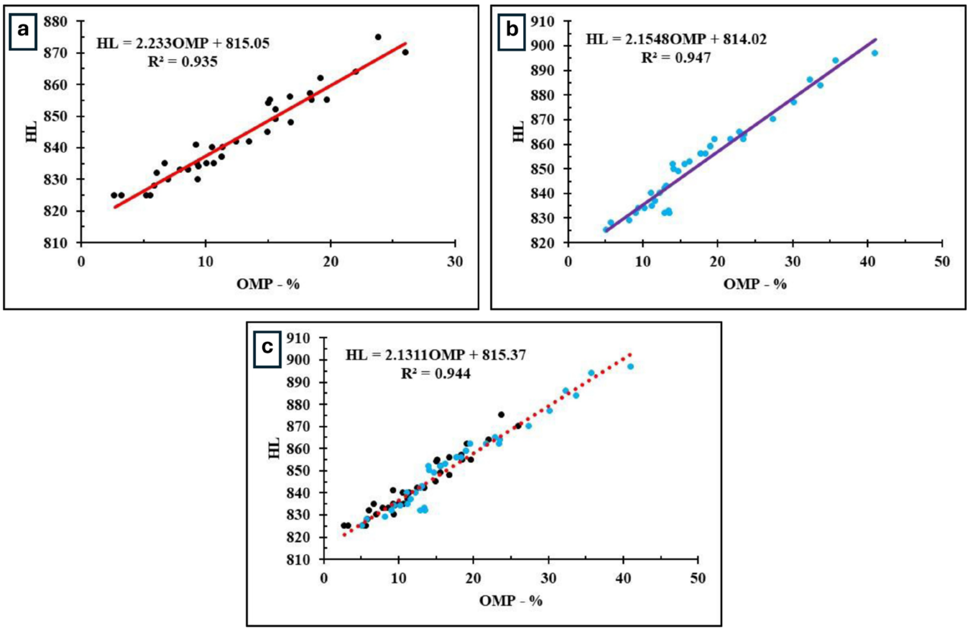

Fig. 4 The relationship between OMP and HL in rocks: (a) Kaman Rose, (b) Dusty Rose, (c) all sample

Previous studies have emphasized that HL values may be influenced by the mineralogical and petrographic composition of the tested surface [7, 31, 38]. However, this issue was first comprehensively investigated in pioneering studies conducted on pyroclastic rocks by Balcı and İnce [32] and İnce et al. [10]. Those studies reported positive linear relationships between lithic fragment content and HL values, whereas negative linear relationships were identified between pumice content and HL values. In the present study, it was determined that increasing orthoclase content in granitic rocks results in increased HL values. The variability in HL values may be associated with differences in the mechanical properties between orthoclase phenocrysts and the surrounding mineral phases, as well as with the heterogeneous character of the rock texture. Variations in mineral hardness, elastic properties, and crystal size may influence rebound behaviour, thereby leading to differences in the measured HL values. Within the scope of this study, the physical properties of the rocks (porosity, dry density, and P-wave velocity) were not directly compared with the HL results. However, it should be noted that the heterogeneous mineralogical and textural structure of phenocryst-bearing rocks may limit the clear identification of the effects of these parameters on HL values.

4 Conclusions

In this study, carried out on granitic rock samples (Kaman Rose and Dusty Rose) collected from two different regions of Anatolia, the effects of the constituent rock-forming minerals on HL values were investigated, and the main findings can be summarized as follows:

The results obtained from both granitic samples demonstrated that the constituent minerals of the rocks, namely orthoclase, plagioclase, quartz, and hornblende, exert a significant control on the measured HL values.

The grain size of orthoclase crystals and their areal proportion on the tested surface, expressed as the orthoclase mineral percentage (OMP), were identified as additional parameters significantly influencing HL values.

A positive linear relationship was established between OMP and HL values for both granite types, with coefficients of determination (R^2) ranging from 0.935 to 0.947. When the entire dataset was evaluated collectively, the corresponding R^2 value was calculated as 0.944.

The findings of this study demonstrate that, for rocks composed of mineral constituents with contrasting mechanical properties, interpretation of HL test results based solely on a single parameter may be insufficient. Accordingly, when applying and interpreting HL tests on rocks exhibiting heterogeneous mineral distributions, both the mineralogical composition and the textural characteristics of the rock should be explicitly taken into consideration. To validate the findings and enhance their generalizability, it is recommended that similar studies be conducted on a larger sample set and that the results be evaluated comparatively.

References

[1] Wakasa, S., Matsuzaki, H., Tanaka, Y., Matsukura, Y. "Estimation of Episodic Exfoliation Rates of Rock Sheets on a Granite Dome in Korea from Cosmogenic Nuclide Analysis", Earth Surface Processes and Landforms, 31(10), pp. 1246–1256, 2006. https://doi.org/10.1002/esp.1328

[2] Mol, L., Viles, H. A. "The Role of Rock Surface Hardness and Internal Moisture in Tafoni Development in Sandstone", Earth Surface Processes and Landforms, 37(3), pp. 301–314, 2012. https://doi.org/10.1002/esp.2252

[3] Wilhelm, K., Viles, H. A., Burke, O., Mayaud, J. "Surface Hardness as a Proxy for Weathering Behaviour of Limestone Heritage: A Case Study on Dated Headstones on the Isle of Portland, UK", Environmental Earth Sciences, 75(10), 931, 2016. https://doi.org/10.1007/s12665-016-5661-y

[4] Kawanishi, T., Hirata, T., Yashiro, T., Kawai, K. "A Simple Method to Evaluate the Depth of Concrete Degradation by Fire", Journal of Advanced Concrete Technology, 17(11), pp. 639–647, 2019. https://doi.org/10.3151/jact.17.639

[5] Wang, Y., Pei, Q., Yang, S., Guo, Q., Viles, H. A. "Evaluating the Condition of Sandstone Rock-Hewn Cave-Temple Façade Using In Situ Non-Invasive Techniques", Rock Mechanics and Rock Engineering, 53(6), pp. 2915–2920, 2020. https://doi.org/10.1007/s00603-020-02063-w

[6] Bembenek, M., Kowalski, Ł., Pawlik, J. "Analysis of the Influence of Surface Roughness of Various Types of Wood on the Results of Their Hardness Measured by the Leeb Method", IOP Conference Series: Materials Science and Engineering, 1199(1), 012071, 2021. https://doi.org/10.1088/1757-899X/1199/1/012071

[7] İnce, İ., Bozdağ, A. "An Investigation on Sample Size in Leeb Hardness Test and Prediction of Some Index Properties of Magmatic Rocks", Arabian Journal of Geosciences, 14(3), 182, 2021.

[8] Gireson, K., Çelik, S. B., Çobanoğlu, İ. "Non-Destructive Estimation of Uniaxial Compressive Strength of Deteriorated Carbonate Building Stones by Frost Action", Environmental Earth Sciences, 82(14), 363, 2023. https://doi.org/10.1007/s12665-023-11032-9

[9] Lobarinhas, R., Dionísio, A., Paneiro, G., Costa e Silva, M. "Evaluating Leeb Hardness as a Reliable UCS Predictor for Stone Masonry Exposed to High Temperatures: The Influence of Porosity Across Diverse Carbonate Lithologies", Journal of Building Engineering, 111, 113079, 2025. https://doi.org/10.1016/j.jobe.2025.113079

[10] İnce, İ., Bozdağ, A., Korkanç, M. "Leeb Hardness Approach in the Determination of Strength after Accelerated Weathering Tests", Studies in Conservation, 70(4), pp. 332–342, 2025. https://doi.org/10.1080/00393630.2024.2382546

[11] İnce, İ., Balcı, M. C., Bozdağ, A., Tosunlar, M. B. "Evaluation of Anisotropy in Rocks Using Non-Destructive Testing Methods", Acta Geodynamica et Geomaterialia, 23(2), pp. 223–264, 2026. https://doi.org/10.13168/AGG.2026.0014

[12] Karakaya, E., İnce, İ. "Prediction of Uniaxial Compressive Strength of Rocks by Non-Destructive Testing via Different Machine Learning Algorithms", Acta Geodynamica et Geomaterialia, 22(3), pp. 303–316, 2025. https://doi.org/10.13168/AGG.2025.0021

[13] Ulusay, R., Ersoy, H., Sünnetci, M. O., Karahan, M. "The Leeb (Equotip) Hardness Test for Rock Materials: An Overview, Assessments on the Factors Influencing Test Results, and Prediction Models Based on a Large Database", Bulletin of Engineering Geology and the Environment, 84(3), 148, 2025. https://doi.org/10.1007/s10064-025-04170-w

[14] Verwaal, W., Mulder, A. "Estimating Rock Strength with the Equotip Hardness Tester", International Journal of Rock Mechanics and Mining Sciences & Geomechanics Abstracts, 30(6), pp. 659–662, 1993. https://doi.org/10.1016/0148-9062(93)91226-9

[15] Meulenkamp, F., Grima, M. A. "Application of Neural Networks for the Prediction of the Unconfined Compressive Strength (UCS) from Equotip Hardness", International Journal of Rock Mechanics and Mining Sciences, 36(1), pp. 29–39, 1999. https://doi.org/10.1016/S0148-9062(98)00173-9

[16] Alvarez Grima, M., Babuška, R. "Fuzzy Model for the Prediction of Unconfined Compressive Strength of Rock Samples", International Journal of Rock Mechanics and Mining Sciences, 36(3), pp. 339–349, 1999. https://doi.org/10.1016/S0148-9062(99)00007-8

[17] Aoki, H., Matsukura, Y. "Estimating the Unconfined Compressive Strength of Intact Rocks from Equotip Hardness", Bulletin of Engineering Geology and the Environment, 67(1), pp. 23–29, 2008. https://doi.org/10.1007/s10064-007-0116-z

[18] Asiri, Y., Corkum, A., El Naggar, H. "Leeb Hardness Test for UCS Estimation of Sandstone", In: Proceedings of the 69th Canadian Geotechnical Conference, Vancouver, Canada, 2016. https://doi.org/10.13140/RG.2.2.27036.90243

[19] Corkum, A. G., Asiri, Y., El Naggar, H., Kinakin, D. "The Leeb Hardness Test for Rock: An Updated Methodology and UCS Correlation", Rock Mechanics and Rock Engineering, 51(3), pp. 665–675, 2018. https://doi.org/10.1007/s00603-017-1372-2

[20] Çelik, S. B., Çobanoğlu, İ. "Comparative Investigation of Shore, Schmidt, and Leeb Hardness Tests in the Characterization of Rock Materials", Environmental Earth Sciences, 78(18), 554, 2019. https://doi.org/10.1007/s12665-019-8567-7

[21] Çelik, S. B., Çobanoğlu, İ., Koralay, T. "Investigation of the Usability of Leeb Hardness Criterion in the Determination of Physicomechanical Properties of Travertine", In: Proceedings of the 26th International Mining Congress and Exhibition of Turkey (IMCET 2019), Antalya, Türkiye, 2019, pp. 577–584. ISBN 978-605-01-1273-3

[22] Yılmaz Güneş, N., Göktaş, R. M. "Comparison and Combination of Two NDT Methods with Implications for Compressive Strength Evaluation of Selected Masonry and Building Stones", Bulletin of Engineering Geology and the Environment, 78(6), pp. 4493–4503, 2019. https://doi.org/10.1007/s10064-018-1382-7

[23] Akbay, D., Ekincioğlu, G. "Estimating the Brittleness Values of Carbonated Rocks with Shore, Schmidt, and Leeb Hardness Values", Environmental Earth Sciences, 81(7), 206, 2022. https://doi.org/10.1007/s12665-022-10332-w

[24] Ghorbani, S., Hoseinie, S. H., Ghasemi, E., Sherizadeh, T. "A Review on Rock Hardness Testing Methods and Their Applications in Rock Engineering", Arabian Journal of Geosciences, 15(11), 1067, 2022. https://doi.org/10.1007/s12517-022-10314-z

[25] Ekincioğlu, G., Akbay, D., Keser, S. "Estimating Uniaxial Compressive Strength of Sedimentary Rocks with Leeb Hardness Using SVM Regression Analysis and Artificial Neural Networks", Politeknik Dergisi, 28(2), pp. 503–512, 2025. https://doi.org/10.2339/politeknik.1475944

[26] Corkum, A. G., Kinakin, D., Séguin, K. "Bayesian Analysis Limitations for Determination of the Unconfined Compressive Strength from Direct and Correlated Indirect Tests", Geotechnical Testing Journal, 49(1), pp. 40–64, 2026. https://doi.org/10.1520/GTJ20250041

[27] Çelik, S. B., Gireson, K. "Development of Nonlinear Regression and Artificial Neural Network Models for Predicting the Uniaxial Compressive Strength of Rocks from Basic Properties and Individual and Integrated Use of Leeb and Schmidt Hardness Measurements", Measurement, 260, 119841, 2026. https://doi.org/10.1016/j.measurement.2025.119841

[28] Ghorbani, S., Hoseinie, S. H., Ghasemi, E., Sherizadeh, T. "Application of Leeb Hardness Test in Prediction of Dynamic Elastic Constants of Sedimentary and Igneous Rocks", Geotechnical and Geological Engineering, 40(6), pp. 3125–3145, 2022. https://doi.org/10.1007/s10706-022-02083-z

[29] Çelik, S. B., Çobanoğlu, İ. "Investigation of the Effect of Saturated Conditions and Number of Measurements on the Leeb Hardness Test and Improved Correlations to Estimate Basic Rock Properties", Acta Geotechnica, 18(8), pp. 4261–4278, 2023. https://doi.org/10.1007/s11440-023-01823-6

[30] Çelik, S. B., Çobanoğlu, İ., Gireson, K. "Prediction and Classification of Flexural Strength of Rock Materials Used as Dimension Stones", Bulletin of Engineering Geology and the Environment, 84(1), 44, 2025. https://doi.org/10.1007/s10064-024-04070-5

[31] Ghorbani, S., Hoseinie, S. H., Ghasemi, E., Sherizadeh, T. "Adoption of ASTM A956-06 Leeb Hardness Testing Standard to Rock Engineering Applications", Construction and Building Materials, 364, 129886, 2023. https://doi.org/10.1016/j.conbuildmat.2022.129886

[32] Balcı, M. C., İnce, İ. "Kayacı Oluşturan Bileşenlerin Leeb Sertliğine Etkisi", Niğde Ömer Halisdemir Üniversitesi Mühendislik Bilimleri Dergisi, 13(4), pp. 1336–1341, 2024. (in Turkish) https://doi.org/10.28948/ngumuh.1523160

[33] Streckeisen, A. "To Each Plutonic Rock Its Proper Name", Earth-Science Reviews, 12(1), pp. 1–33, 1976. https://doi.org/10.1016/0012-8252(76)90052-0

[34] TS "TS EN 1936, Natural Stone Test Methods – Determination of Real Density and Apparent Density and of Total and Open Porosity", Turkish Standards Institution, Ankara, Türkiye, 2010.

[35] ASTM "ASTM E494-20, Standard Practice for Measuring Ultrasonic Velocity in Materials", ASTM International, West Conshohocken, PA, USA, 2020. https://doi.org/10.1520/E0494-20

[36] ASTM "ASTM A956/A956M-22, Standard Test Method for Leeb Hardness Testing of Steel Products", ASTM International, West Conshohocken, PA, USA, 2022. https://doi.org/10.1520/A0956_A0956M-22

[37] TS "TS EN 12407, Natural Stone Test Methods – Petrographic Examination", Turkish Standards Institution, Ankara, Türkiye, 2019.

[38] Çelik, S. B., Çobanoğlu, İ., Koralay, T., Gireson, K. "Investigation of the Leeb Hardness Test in Rapid Characterisation of Rock Cores with Particular Emphasis on the Effect of Length to Diameter Ratio", International Journal of Mining, Reclamation and Environment, 37(7), pp. 524–543, 2023. https://doi.org/10.1080/17480930.2023.2213549